

## **The Modelling of Stable and Metastable Phase Formation in Multi-Component Al-Alloys**

N. Saunders

Thermotech Ltd., Surrey Technology Centre, The Surrey Research Park  
Guildford, Surrey GU2 7YG, U.K.

Keywords: Alloy constitution, metastable phases, TTT diagrams, solidification, CALPHAD.

### **Abstract**

In recent years the use of thermodynamic modelling via the CALPHAD method has been extensively applied to industrial alloys of many types. Although pertaining to equilibrium conditions, valuable information can be gained for a variety of practical applications where equilibrium is not reached, for example, in solidification. The purpose of the present paper is to provide a review and examples of the practical application of the CALPHAD method to commercial industrial alloys. A further purpose of the paper is to present new results for the modelling of metastable hardening phases, such as GP zones,  $\theta'$ ,  $S'$ ,  $Mg_xSi_y$  based phases, and show how CALPHAD modelling can be extended to calculate relevant TTT and CCT diagrams for their formation.

### **1. Introduction**

For many years the prime sources of information regarding phase equilibria in Al-alloys have been the compendia of Philips [1] and Mondolfo [2]. These books provide extensive information concerning the behaviour of binary and ternary systems and, to a certain degree, higher order systems. Such work enables a reasonable understanding of many known alloys. However, while providing broad information on particular alloy systems, equilibrium phase diagrams fall short in providing detailed information on how multi-component alloys behave, particularly for the case of new alloys and in understanding what may happen as compositions vary within the composition specification of known alloys.

Recently, the use of thermodynamic calculations via the CALPHAD method [3] has demonstrated that high quality calculations can be made for complex alloys of many types, including Al-based alloys. In particular, phase formation in numerous types of Al-alloy is well matched [4,5] and the approach is readily extendable to use in solidification modelling [4,6]. The aim of the present paper is to review past work and present the present status of CALPHAD calculations to Al-alloys and their extension to modelling of solidification. It will also present new work concerning the modelling of metastable phases and their transformation kinetics.

## 2. Background

Thermodynamic calculations have often been perceived as rather theoretical and applicable only to simple systems. However, verification of CALPHAD predictions against multi-component alloys of many types has shown that they provide results that are very close to experimental observation [3]. It is only in recent years that attempts have been made to calculate phase equilibria for multi-component Al-alloys. Previous work had tended to rely on modelling binary and ternary sub-systems, but this position has changed and predictions for complex Al-alloys can now be routinely performed [4,5, 7].

Well established models have been developed that can be used to describe the thermodynamic properties of many different types of phase [3,8,9,10]. All types of models require input of coefficients that uniquely describe the properties of the various phases and these coefficients are held in databases, which are either in the open literature or proprietary. These databases are then accessed by software that performs Gibbs energy minimisation and complex multi-component calculations can be performed. There are now a variety of software packages for doing such calculations. Bale and Eriksson [11] provided a fairly comprehensive coverage of these circa 1990, while a recent issue of CALPHAD [12] provides details of some newer software programmes.

The roots of the CALPHAD approach lie in the mathematical description of the thermodynamic properties of the phases of interest. If they are stoichiometric compounds their composition is defined and a mathematical formula is then used to describe fundamental properties such as enthalpy and entropy. Where phases exist over a wide range of stoichiometries, which is the usual case for metallic materials, other mathematical models are used which account for the effect of composition changes on Gibbs energy.

A strength of the CALPHAD method is that it is based on predicting the thermodynamic properties of the higher-order system from those of the lower-component binary and ternary systems. This provides a very powerful methodology as information from binaries and ternaries can be used directly towards a quantitative prediction of multi-component behaviour.

Most thermodynamic models for the Gibbs energy of a phase ( $G$ ) can broadly be represented by the general equation

$$G = G^o + G_{mix}^{ideal} + G_{mix}^{xs} \quad (1)$$

where  $G^o$  is a reference state, usually linked to the Gibbs energy of the phase in its pure form,  $G_{mix}^{ideal}$  is the ideal mixing term and  $G_{mix}^{xs}$  is the excess Gibbs energy of mixing of the components. The main solution phase models used for Al-alloys are the substitutional type model and the multiple sublattice model [3]. It is not within the scope of the present paper to describe in detail these models, particularly the multiple-sublattice model, but it is useful to briefly discuss some of their aspects.

The Gibbs energy of a substitutional phase in a many component system can be represented by the equation

$$G = \sum_i x_i G_i^o + RT \sum_i x_i \ln x_i + \sum_i \sum_j x_i x_j \sum_v \Omega_v (x_i - x_j)^v \quad (2)$$

where  $x_i$  is the mole fraction of component  $i$ ,  $G_i^o$  is the Gibbs energy of the phase in the pure component  $i$ ,  $T$  is the temperature and  $R$  is the gas constant.  $\Omega_v$  is an interaction coefficient dependent on the value of  $v$ . When  $v$  is limited to a value of 0, this corresponds to the regular solution model and when values for 0 and 1 are provided, this corresponds to a sub-regular type model. In practice values for  $v$  does not usually rise above 2.

Eq.2 assumes higher order interactions are small in comparison to those arising from the just the binary terms but this may not always be the case. Ternary interactions are often considered, but there is little evidence of the need for interaction terms of a higher order than this. Various other polynomial expressions for the excess term have been considered. However all are based on predicting the properties of the higher-order system from the lower-component systems.

The multi-sublattice model is substantially more complex and considers the phase to be made up of multiple interlocking sublattices. There are then interaction terms to be considered (i) between the sublattices and (ii) on the sublattices themselves. Full descriptions of such models, as well as further reading, can be found in [3].

Because of the importance of the lower order calculations it is instructive to view typical results for two binary and ternary systems (Figs.1-4) before proceeding to the main part of the paper concerning applications to multi-component alloys. Figures 1 and 2 show, respectively, calculations for the Al-rich part of the Al-Cu phase diagram and the Al-Mg phase diagram. Figure 3 shows the combination of these two diagrams (along with a model for the Cu-Mg system) to calculate the ternary system Al-Cu-Mg. In this case modelling must concern itself with ternary phases and the accuracy to which this can be done is a cornerstone of the modelling of Al-Alloys. Figure 4 shows the liquidus projection for the Al-Mn-Si ternary system. Once the relevant binary and ternary thermodynamic assessments are made it is possible to advance to multi-component alloys.

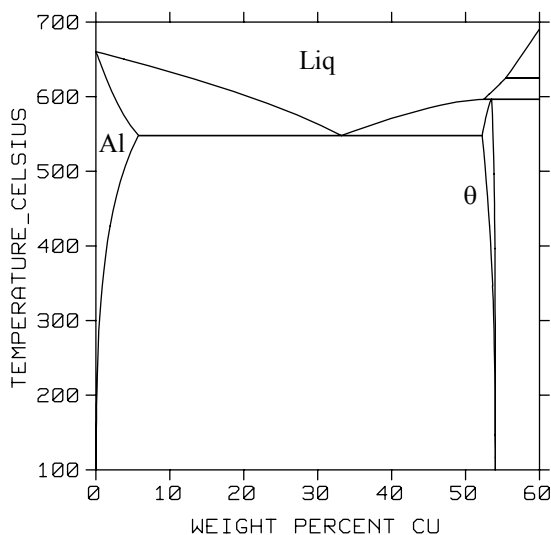


Figure 1: Calculated Al-Cu phase diagram

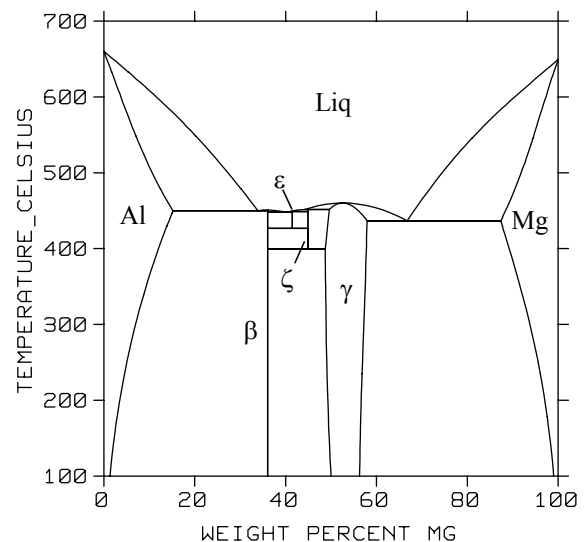


Figure 2: Calculated Al-Mg phase diagram

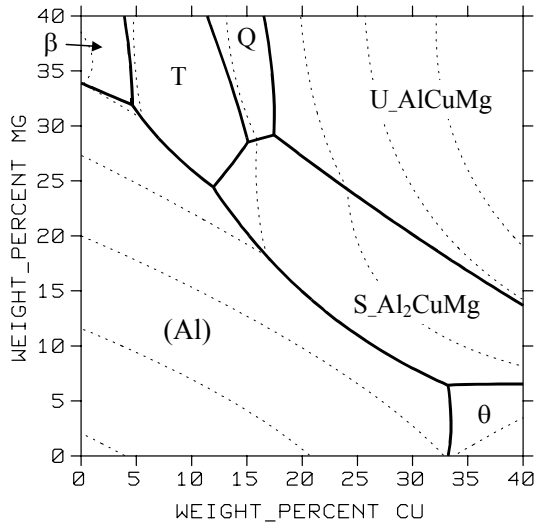


Figure 3: Calculated liquidus projection for Al-Cu-Mg

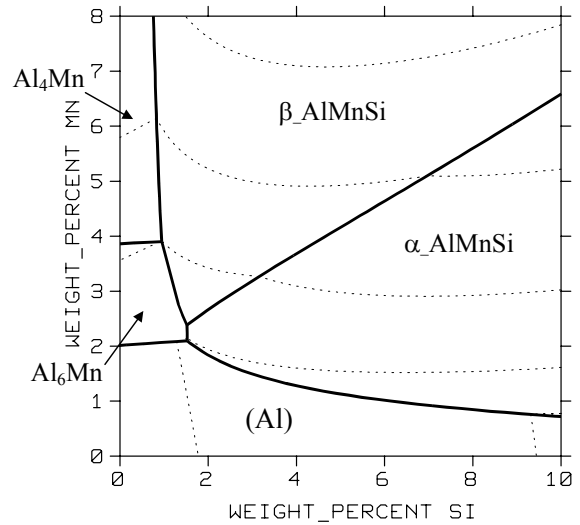


Figure 4: Calculated liquidus projection for Al-Mn-Si

### 3. Applications

#### 3.1 Stable Phase Equilibria calculations

While diagrams such as those shown in Figure 1-4 are the most commonly associated with phase equilibria, they are very limiting when it comes to understanding what will happen in multi-component alloys. It is often far more useful to show plots of a property vs. temperature. For example, plots of the amount of phase vs. temperature are often the most commonly used diagrams for multi-component calculations. Also, the composition of a phase as a function of temperature is regularly used. Examples of such calculations are shown in Figures 5 and 6.

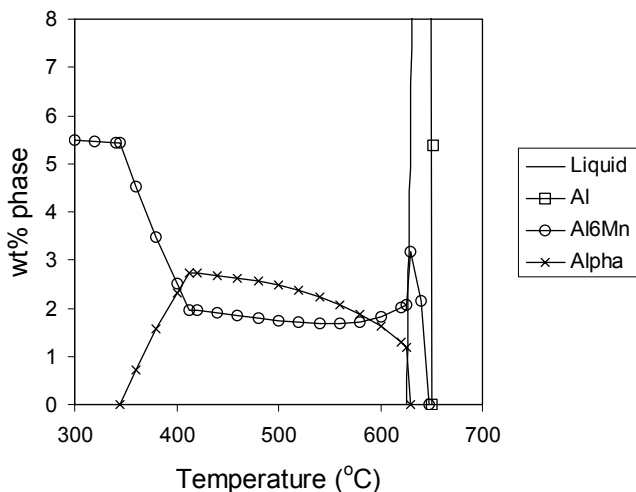


Figure 5: Calculated phase % vs. temperature plot for an AA3104 alloy

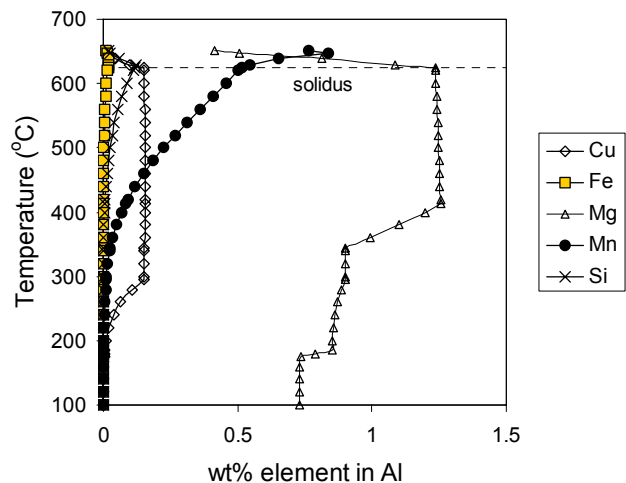


Figure 6: Calculated solubility of alloying elements in Al for an AA3104 alloy

Figure 5 shows the equilibrium phases in an AA3104 alloy. In this case the predominant phase to be formed during casting is the  $Al_6Mn$  phase. The peritectic reaction that forms  $\alpha-AlFeMnSi$ , at the expense of  $Al_6Mn$ , is usually incomplete after solidification and the alloy contains predominantly  $Al_6Mn$ . However, during solution treatment there is sufficient time

for the transformation to occur and most of the  $Al_6Mn$  transforms to  $\alpha$ . The degree to which  $\alpha$  predominates is sensitive to alloy composition, particularly to Si. The desirability of forming the  $\alpha$  phase in preference to  $Al_6Mn$  is well documented, as is the importance of Si on this transformation [13]. Figure 6 shows the solubility of the various elements in AA3104 in Al. This type of diagram is quite an attractive option as the maximum solubility of elements such as Mn and Si can be clearly seen as well as the solubility curve for each element as a function of temperature.

The above alloy is quite a simple type and it is possible to look at very complex alloys such as those from the 7XXX series. In these alloys a variety of phases can form, some of which are detrimental, while others are desirable. The calculated phase % vs. temperature plot for the well known alloy AA7075 is shown Figure 7 and accurately reflects the phases that are observed in the alloy [14]. Figure 8 shows the solubility of various elements in Al. In this case, the levels of the major alloying elements change more markedly with temperature. This has a major subsequent effect on the properties of the Al phase itself, for example in electrical and thermal conductivity as well as inherent strength.

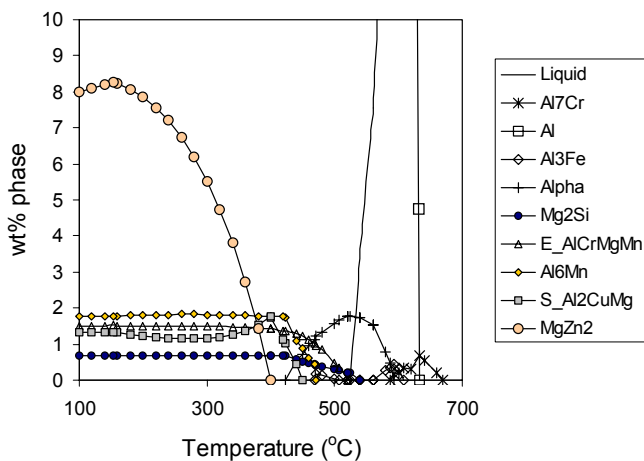


Figure 7: Calculated phase % vs. temperature plot for an AA7075 alloy

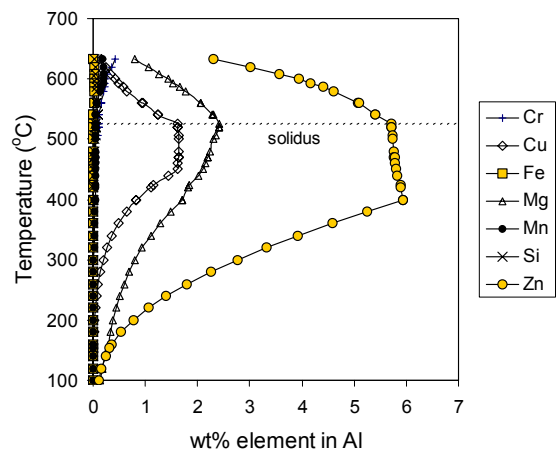


Figure 8: Calculated solubility of alloying elements in Al for an AA7075 alloy

### 3.2 Metastable Phase Equilibria calculations

The alloy AA7075 highlights one of the limitations with *equilibrium* calculations, in that the phases formed may not be those predicted to be in equilibrium. As it turns out, for many cases, equilibrium calculations provide valuable information for processing, liquidus and solidus temperatures, solubility curves etc.. However, many Al-alloys are hardened by metastable phases such as  $\theta'$ ,  $S'$ ,  $\eta'$ , GP zones etc.. It is therefore important that the thermodynamic calculations are able to include such phases, both for understanding and predicting metastable equilibria, but also as necessary input into kinetic equations to calculate the conditions for formation of these phases. To this end, work has been undertaken to thermodynamically characterise the important metastable hardening phases in Al-alloys.

It is possible to make metastable equilibrium calculations using the CALPHAD route by excluding certain stable phases in the calculation and allowing the software to calculate a metastable equilibrium. General features of such calculations are given in Saunders and Miodownik [3].

For Al-alloys, GP zones are of great importance and work has been undertaken to model their thermodynamic properties. The current thermodynamic model is based on the premise that GP zones are formed due to a metastable miscibility gap in the Al-rich FCC phase. Such an approach has been postulated by Murray [15] for GP zones in Al-Cu, and Löffler et al. [16] with respect GP zone formation in Al-Zn-Mg alloys. For the case of GP zone formation in Al-Cu we observe, as did Murray, that the straightforward calculation of the miscibility gap produces solvus temperatures for GP zone formation that are substantially higher than observed in practice. Following Murray, this is considered due to the high elastic strain energy that exists at the coherent interface between the Al-rich FCC phase and the Cu-rich GP zone. This has the effect of depressing the solvus temperature and a term, proportional to the concentration of Cu in the GP zone, has been included in the thermodynamic description to empirically account for this elastic strain energy contribution. Otherwise, the calculation for GP zones considers a straightforward miscibility gap in the FCC phase.

Based on an assessment of observed temperatures of formation of the various other types of metastable hardening phase, thermodynamic parameters have been evaluated for  $\theta'$ , various  $Mg_xSi_y$  phases, and the metastable forms of the T, S and  $MgZn_2$  stable phases,  $T'$ ,  $S'$  and  $\eta'$ . Detailed information exists for solvus temperatures of GP zones in Al-Cu [17,18,19,20] and Al-Mg-Zn alloys [16], as well as for  $\theta'$  [19,21,22] and Figure 9 shows a comparison between observed solvus temperatures and those calculated using the present model. There is a discrepancy between calculation and results of Matsuyama [21] for  $\theta'$  at low solvus temperatures. To obtain a better agreement requires an unrealistic entropy of formation for  $\theta'$ . Such problems are usually associated with equilibrium (or in this case metastable equilibrium) not being achieved at low temperatures.

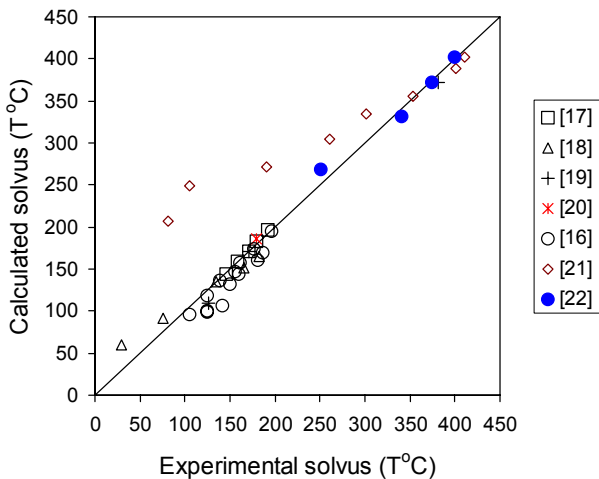


Figure 9: Comparison between experimental and calculated solvus temperatures for GP zones in Al-Cu and Al-Mg-Zn and for the  $\theta'$  phase in Al-Cu.

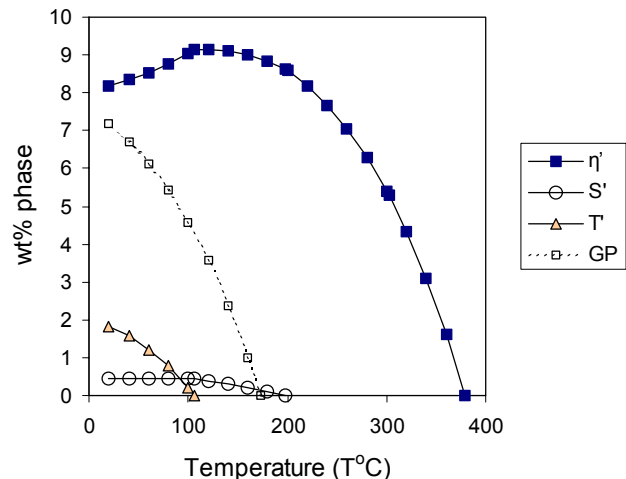


Figure 10: Calculated phase % vs. temperature plot for the metastable phases in an AA7075 alloy. GP calculation made assuming  $T'$ ,  $S'$  and  $\eta'$  are not formed.

Figure 10 shows a plot of metastable hardening phases,  $S'$ ,  $T'$  and  $\eta'$ , in AA7075 as a function of temperature. The calculation has been made on the following basis: (1) It is assumed that the metastable phases will form from the Al phase quenched from the solution treatment temperature. Therefore, the calculation has been made with the composition of Al at this temperature. (2) The stable phases have not been included in the calculation. While correctly predicting that the  $\eta'$  phase will form in substantial amounts, GP zones are not calculated as they are themselves metastable with respect to  $\eta'$ ,  $T'$  and

S'. In order to calculate the curve for GP zones, it is necessary to suspend  $\eta'$ ,  $T'$  and  $S'$  from the calculations and make a calculation for the metastable equilibrium between Al and the GP zones. This is also shown in Figure 10. However, the limitations of a purely thermodynamic approach are becoming apparent. Too many assumptions need to be made and it is clear that any useful understanding of metastable phases is inherently tied to their kinetics of transformation. This issue will be dealt with in Section 3.4

### 3.3. Solidification modelling

A now widespread use of CALPHAD modelling for Al-alloys is the calculation of phase formation during solidification [4,6,23]. In particular, highly useful information can be gained for process modelling, in that heat evolution as a function of fraction solid formed is a key input for heat flow in casting simulations. This is achieved by the implementation of simple kinetic model based on the so-called Scheil-Gulliver (SG) concept.

The SG model can be considered as a complementary limiting case to equilibrium solidification whereby it is assumed that solute diffusion in the solid phase is small enough to be considered negligible and that diffusion in the liquid is extremely fast, fast enough to assume that diffusion is complete. Based on the premise that liquidus and solidus lines are linear, the composition of solid formed during solidification ( $C_s$ ), as a function of the fraction of solid formed ( $f_s$ ) can be expressed as

$$C_s = kC_o(1-f_s)^{k-1} \quad (3)$$

where  $C_o$  is the composition of the alloy and  $k$  is the partition coefficient. From this the fraction solid formed as a function of temperature is given by

$$f_s = 1 - \left( \frac{T_f - T}{T_f - T_L} \right)^{\left[ \frac{1}{k-1} \right]} \quad (4)$$

where  $T_L$  and  $T_f$  are the liquidus and solidus temperature. The treatment above is the traditional derivation of the Scheil equation but it has quite severe restrictions when applied to multi-component alloys. It is not possible to derive this equation, using the same mathematical method, if the partition coefficient,  $k$ , is dependent on temperature and/or composition. The Scheil equation is applicable only to dendritic solidification and cannot, therefore, be applied to eutectic alloys that are common type for Al-alloys. Further it cannot be used to predict the formation of intermetallics during solidification.

Using thermodynamic modelling all of the above disadvantages can be overcome. The process that physically occurs during 'Scheil' solidification can be envisaged as follows. A liquid of composition  $C_o$  is cooled to a small amount below its liquidus. It precipitates out solid with a composition  $C_{S,1}$  and the liquid changes its composition to  $C_{L,1}$ . However, on further cooling the initial solid cannot change its composition due to lack of back diffusion and it is effectively 'isolated'. A local equilibrium is then set up where the liquid of composition  $C_{L,1}$  transforms to a liquid of composition  $C_{L,2}$  and a solid with composition  $C_{S,2}$ , which is precipitated onto the original solid with composition  $C_{S,1}$ . This process occurs continuously during cooling and when  $k < 1$  leads to the solid phase being lean in solute in the center of the dendrite and the liquid becoming more and more enriched in solute as solidification proceeds. Eventually, the composition of the liquid will reach the eutectic composition and final solidification will occur via this reaction.

Any appearance of secondary phases can be easily taken into account in this approach with the assumption that no back diffusion occurs in them. Therefore, all transformations can be accounted for, including the final eutectic solidification. The approach described here is based on an isothermal step process but, as the temperature step size becomes small, it provides results that are almost completely equivalent to those which would be obtained from continuous cooling. A further and very significant advantage of using a thermodynamic approach is that the heat evolution during solidification is a straightforward product of the calculation. The limit to the SG simulation is that some back diffusion will take place. However, if the degree is small, good results will still be obtained. Backerud et al. [24] have experimentally studied almost 40 commercial alloys and calculated results have been compared to all of these. Results of the comparisons of fraction solid vs temperature for some of these alloys are shown in Fig.11. The agreement is most striking and the level of accuracy achieved for these alloys is quite typical of that attained overall in the comparison.

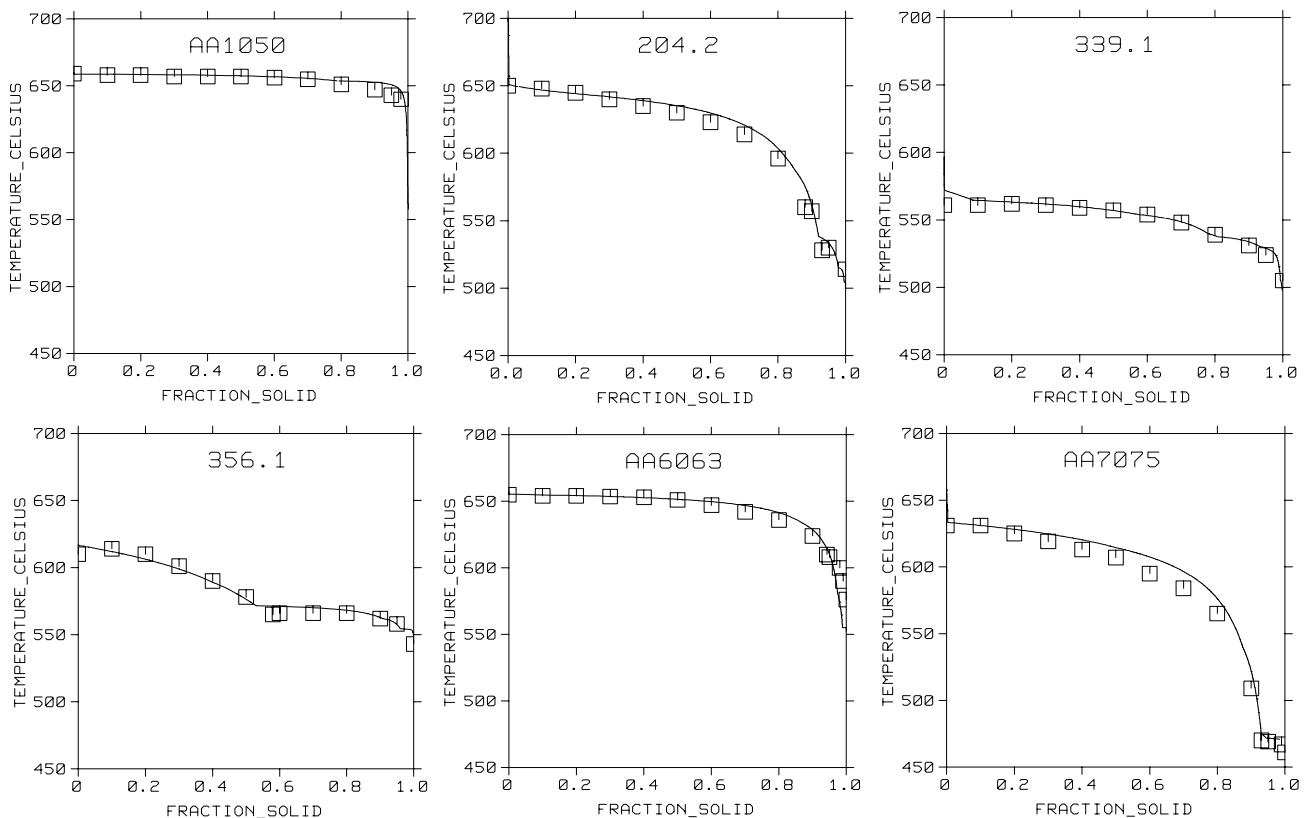


Fig.11 Fraction solid vs. temperature plots for various Al-alloys calculated under 'Scheil' conditions with experimental results ( $\square$ ) of Backerud et al [24] shown for comparison.

### 3.4 TTT and CCT diagrams for Al-alloys

As shown in section 3.2, thermodynamic descriptions are now available for many of the important metastable strengthening phases in Al-alloys. The key to making the modelling useful is to couple the thermodynamic descriptions with kinetic models so that rates of transformation can be calculated. This has been done using a model that has been generally applied to other alloy types, such as stainless steels, Ni-based and Ti-based alloys [25,26,27,28]. The kinetic treatment is based on a modified Johnson-Mehl-Avrami model where critical input such as driving forces, compositions of the precipitating phases

are obtained from a thermodynamic calculation. Work has been undertaken to build up the requisite diffusion databases, assess the typical nucleation and shape characteristics for the various types of precipitate, and validate the approach by comparison with experiment. An advantage of the current modelling method is that few input parameters need to be empirically evaluated. Where empirical values are used, for example in consideration of shape and nucleant density, specific values have been defined for the various precipitates. Once these values are defined, they have then been self-consistently applied and the model can therefore be used in a predictive fashion.

In terms of kinetics, Al-alloys potentially present a special case. Solution temperatures are close to melting temperatures and consequently there are large numbers of equilibrium vacancies. On quenching these may be retained leading to considerably enhanced diffusion processes at precipitation temperatures. To this end the diffusion equation used in the current model considers that the equilibrium concentration of vacancies present at the solution treatment temperature is retained to low temperatures. Based on this assumption, it is possible to calculate TTT and CCT diagrams that provide good quality representations of the behaviour of Al-alloys. It is understood that certain heat treatment processes rely on indirect ageing methods, in which case GP zones may form as an intermediate stage in the hardening process. It is not possible at this current time to deal with this case. Nonetheless, important information concerning heat treatment for many alloys can be gained from such TTT and CCT diagrams.

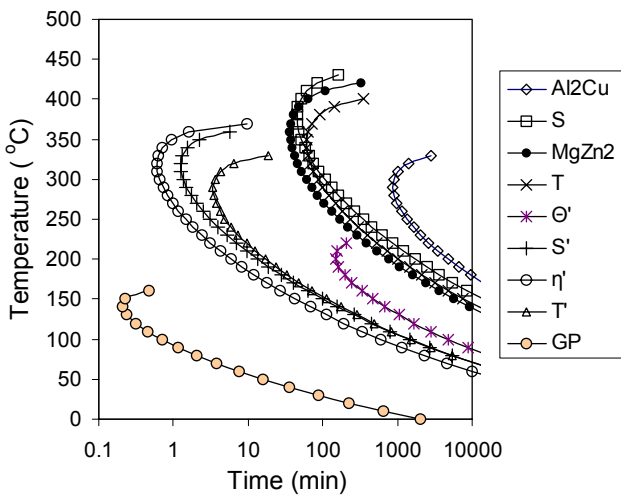


Figure 12: Calculated TTT diagram for AA7075

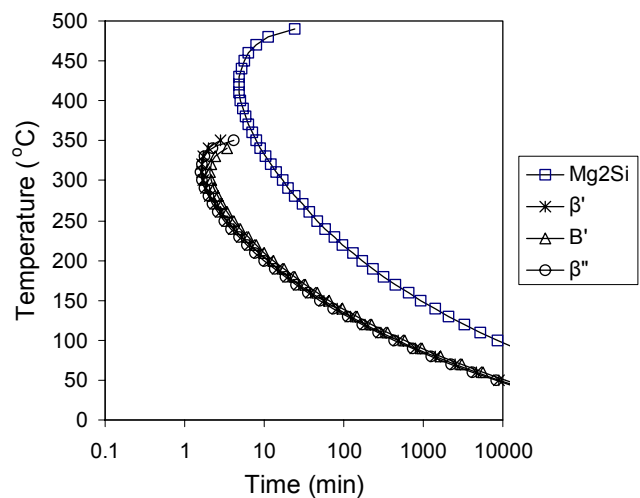


Figure 13: Calculated TTT diagram for AA6061

The model has been included in the software programme JMatPro [25,28], which has been used to calculate the relevant TTT and CCT diagrams shown in the present paper. Figure 12 shows the TTT diagram calculated for AA7075 for start of transformation of various phases from the supersaturated Al phase. We have used 0.5% amount of phase formed as generally corresponding to the start of noticeable transformation. In some cases measurement techniques may be very sensitive and a value of 0.1% may be more appropriate, but otherwise practice shows 0.5% is a reasonable value to take for general purposes. The behaviour appears to match experimental observation in all aspects. At temperatures below 170°C, GP zone formation is favoured and kinetics are rapid at normal 1<sup>st</sup> stage annealing temperatures of 100-120°C. Furthermore, it is clear from Figure 10 that overaging will cause the GP zones to transform to the more stable  $\eta'$  and 2<sup>nd</sup> stage heat treatment at typical temperatures of 160-180°C will accelerate this process. Figure

13 shows a TTT diagram for an AA6061 alloy that is hardened by  $Mg_xSi_y$  metastable phases. Times for onset of transformation are again very consistent with strength vs. time behaviour at various temperatures [29,30] The stoichiometries of these phases have been taken after Edwards et al. [31] as well as the nomenclature  $\beta'$ ,  $\beta''$  and  $B'$ . In the calculated TTT diagram there is extremely close competition between the various  $Mg_xSi_y$  forms. In such a case, small variations in nucleant site densities may cause one type to predominate, which is difficult to accommodate in the kinetic model in a self-consistent fashion. However, it is clear in such alloys that it is quite common for the various forms to co-exist, which is consistent with the current calculation.

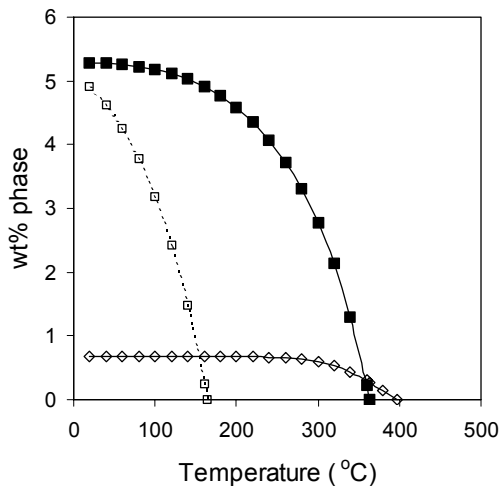


Figure 14: Calculated phase % vs. temperature plot for the metastable phases in a 319 alloy. GP calculation assumes  $\theta'$  and  $B'$  are not formed.

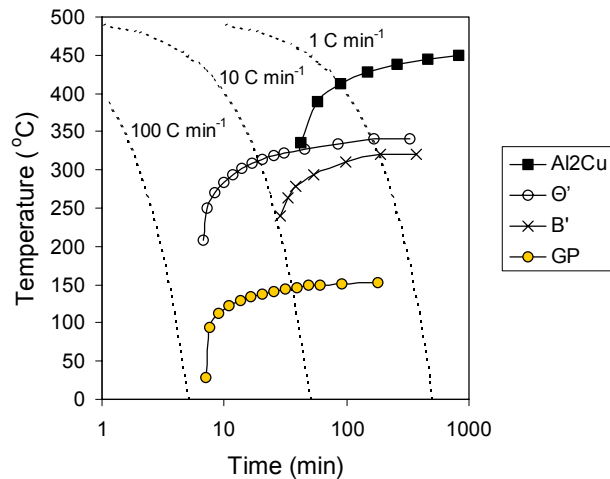


Figure 15: Calculated TTT diagram for a 319 alloy

In casting alloys the CCT behaviour can be of critical importance. To this end a 319 casting alloy has been taken and the precipitation behaviour from the Al phase modelled after solution treatment at 500°C. Figure 14 shows the metastable phases that exist in the alloy, with the  $\theta'$  predominating with a very small amount of  $B'$  potentially present. GP zone formation is also shown. The alloy can be considerably hardened by  $\theta'$  [32] consistent with calculation. The cooling rate from the solution temperature can substantially vary in engine parts, where 319 is used, and it becomes important to know the critical cooling rates that will ensure full hardening can occur without the formation of large stable intermetallics that may appear if cooling rates become too slow [32]. Figure 15 shows the calculated CCT curve for the alloy demonstrating that for a wide range of cooling rates the stable  $Al_2Cu$  can be avoided, as found in practice.

## Summary

Thermodynamic modelling techniques have now advanced sufficiently so that they can be used as a powerful tool in understanding both stable and metastable phase formation in multi-component Al-alloys. Their use in practice has been demonstrated both for solid state transformations and for solidification. The present paper provides examples of CALPHAD calculations for stable phase formation in the solid state and a simple extension to model non-equilibrium phase formation in solidification. The paper also presents, for the first time, publication of results for the modelling of the various metastable hardening phases in multi-component alloys with the subsequent extension to the kinetic modelling of

phase formation in Al-alloys, with particular respect to the formation of GP zones,  $Mg_xSi_y$  metastable phases,  $\theta'$ ,  $S'$ ,  $\eta'$  etc.. Results of the kinetic modelling show excellent consistency with observed behaviour in practice.

### Acknowledgements

The author gratefully acknowledges the guidance and help in preparation of this paper from Dr. Zhanli Guo and Dr. Jean-Philippe Schillé and Prof. Peter Miodownik. Figures 1-4 have been calculated by Thermo-Calc [33], while Figures 5-15 have been calculated using JMatPro [25,28].

### References

- [1] H.W.L. Phillips, Equilibrium Diagrams of Aluminium Alloy Systems, The Aluminium Development Assoc., London, UK, 1961.
- [2] L.F. Mondolfo, Aluminium Alloys: Structure & Properties, Butterworths, London, 1976.
- [3] N. Saunders and A. P. Miodownik, CALPHAD – Calculation of Phase Diagrams, Pergamon Materials Series vol.1, ed. R. W. Cahn, Elsevier Science: Oxford, 1998.
- [4] N. Saunders, J.JILM, 51, 141, 2001.
- [5] P. Kolby, Proc. 4th Int. Conf. on Al-alloys: Their Physical and Mechanical Properties, vol.3, eds. T.H. Sanders Jr. and E.A. Starke Jr., Georgia Institute of Technology, 2, 1994.
- [6] N. Saunders, Light Metals 1997, ed. R. Huglen, Warrendale, PA: TMS, 911, 1997.
- [7] L. Kaufman: Computer Aided Innovation of New Materials II, (eds.M. Doyama, J. Kihara, M. Tanaka and R. Yamamoto), Elsevier Science, Amsterdam, (1993), 683.
- [8] M. Hillert: Computer Modelling of Phase Diagrams, (ed.L.H.Bennett), TMS, Warrendale, PA, 1, 1986.
- [9] G. Eriksson and K. Hack: Met. Trans. B, 21B (1990), 1013.
- [10] I. Ansara, Int.Met.Reviews, 22, 20, 1979.
- [11] C. W. Bale and G. Eriksson: Canadian Met. Quarterly, 29 (1990), 105.
- [12] CALPHAD, 26(2), 2002.
- [13] G.J. Marshall, Mater. Sci. Forum, 217-222, 19, 1996.
- [14] Metals Handbook, 9<sup>th</sup> Ed., ASM, Metals Park, OH, 9, 351, 1985.
- [15] J.L. Murray, Int. Met. Reviews, 30, 211, 1985.
- [16] H. Löffler, I. Kovács and J. Lendvai, J. Mater. Sci., 18, 2215, 1983.
- [17] R.H. Beton and E.C Rollason, J. Inst. Met., 86, 1957-58.
- [18] R. Baur and V. Gerold, Z. Metallkde., 57, 181, 1966.
- [19] R. Baur, Z. Metallkde., 57, 275, 1966.
- [20] K.G. Satyanarayana, K. Jayapalan and T.R. Ananthraman, Current Sci., 42, 6, 1973.
- [21] K. Matsuyama, Kinzoku-no Keyu, 11, 461, 1934.
- [22] G. Borelius, J. Anderson and K. Gullberg, Ing. Vetenskaps Akad. Handl., 169, 5, 1943.
- [23] N. Saunders, X. Li, A.P. Miodownik and J.-Ph. Schillé, Light Metals 2003, ed. P. Crepeau, TMS, Warrendale, PA, 999, 2003.
- [24] L. Backerud, E. Krol and J. Tamminen, Solidification Characteristics of Aluminium Alloys: Vols.1 and 2, Tangen Trykk A/S, Oslo, 1986
- [25] N. Saunders, X. Li, A.P. Miodownik and J-Ph. Schillé, Materials Design Approaches and Experiences, eds. J.-C. Zhao et al., TMS, Warrendale, PA, 185, 2001.
- [26] X. Li, A.P. Miodownik and N. Saunders, Mater. Sci. Tech., 18, 861, 2002.
- [27] N. Saunders, X. Li, A. P. Miodownik and J.-Ph. Schille, to be published in Proc. Conf. Ti-2003, Hamburg, July, 2003
- [28] N. Saunders, Z. Guo, X. Li, A. P. Miodownik and J-Ph. Schillé, JOM, December, 60, 2003.
- [29] Metals Handbook 10<sup>th</sup> Ed., ASM, Metals Park, OH, 2, 29, 1990.
- [30] S.K. Varma, J. Ponce, S. Edwards, E. Corral and Daniel Salas, Mater. Sci. Forum, 217-222, 931, 1996
- [31] G.A. Edwards, K. Stiller, G.L. Dunlop and M.J. Couper, Mater. Sci. Forum, 217-222, 713, 1996.
- [32] J. Allison, presented at Int. Symp. Accelerated Implementation of Materials & Processes, Chicago, IL, Nov.10-12, 2003
- [33] J.-O. Anderson, T. Helander, L. Höglund, P. Shi and B. Sundman, CALPHAD, 26, 273, 2002